Bu-Ali Sina University

Optimization of a Reinforced-flat End Cap Through Analytical Study and Genetic Algorithm

A.R. Hosseinzadeh*, M. Ebrahimi, H. Sodagari, A.R. Abedian

Air Cooled Condensate Group, Mechanical Engineering Department, Monenco Iran Consulting Engineers, Iran.

Article info	Abstract

An efficient design is a key factor in final expenditure of a certain construction. Pressure vessels are structures that play an indispensable role in different industries such as petroleum, power plants etc. Pressure vessels are receptacles often used to keep gases or liquids at a pressure typically different from what atmospheric pressure is. End caps which close the end of vessels can be formed in different shapes. Thus, end cap design also has a significant role in the integrity of vessels to prevent fatal accidents that are frequent in the pressure vessel's history. In this study, an extensive investigation of huge-flat end caps under external pressure was carried out to extract the most efficient geometrical layout. This kind of flat end cap is an essential part of the designed main duct in the Air Cooled Condenser (ACC) systems as a configuration that renders steam to condensed water inside a definite arrangement of finned tubes in a hybrid thermal power plant. To determine an optimized state of stresses considering weight limitation, a number of finite element models were simulated. The simulations were performed in a relatively wide domain of two geometrical variables, namely thickness and height of stiffeners. By constituting a comprehensive data library, an objective function was formed using the results of finite element. The procedure was followed through a genetic algorithm to find an optimized stress state. An analytical study was also accomplished to reach an optimized end cap resulting in the lowest stress level. The findings showed very similar results for the two methods. Furthermore, a profound observation of the influence of two geometrical parameters was conducted in different weight limits. Although this study is based on a particular actual-industrial problem in an implemented power plant, the proposed method and results are applicable to a great number of similar cases.

1. Introduction

Pressure vessels are extensively employed in industries for processing and storage of fluids and steams at different operating temperatures and pressures. Storage and transportation tanks, thin and thick-walled vessels, are the most frequent types of vessels. If the diameter of vessel is equal to or more than 10 times the thickness of the wall, it is typically called thin-walled vessels; otherwise it is known as thick-walled. Storage tanks are usually known for their significantly thin walls, it is for the simple reason that the dead-sustained loads are the only ones that they are capable to tolerate. Vessels for transportation are thin-walled ones produced in large size [1]. Appropriate design procedure has a significant importance in protecting the vessels from

explosion which could lead to injury of humans and also destruction of designed setups. Although an appropriate design requires a reasonable range of stresses [2], an economic design is worthwhile through reducing the weight of structures. Therefore, making an appropriate compromise between weight and stresses is a challenge during engineering designs.

A spherical shape is the most reliable configuration for a pressure vessel. Inherently, the pressure inside a pressure vessel tries to bend the walls out. Thus, due to its symmetrical and subsequently stable shape, a spherical vessel is claimed to be able to tolerate the most internal and external loads [3]. In spite of merits involved with using spherical vessel, its producing is rather formidable and not economical. As a consequence, the majority of pressure vessels are formed in shape of cylinder which can be equipped with different types of caps on each end. At the same time, end cap plays a significant role in the lifetime of the entire vessel's structure and its integrity. These end caps are typically categorized as ellipsoidal, spherically dished (torispherical), hemispherical, conical, tori-conical and flat ones. The internal capacity of end caps is directly related to the cost of each type of end cap. In this way, hemispherical end caps have greater internal volumes compared to ellipsoidal ones, which have greater internal volumes than spherically dished end caps. Blunt or flat end cap is the most critical type of the end caps whose design needs a careful examination. Undoubtedly, the optimum design can be accomplished through the use of a correct arrangement of reinforcement. It is also noteworthy to mention that vessels under external pressure shall meet more requirements in comparison with internal-pressured vessels [4]. In the current study, the former type has been focused on.

Hassan et al. [5] has proposed a method for optimization of pressure vessels by investigating numerous parameters such as thickness, length and radius of the shell through a rather new technique called Ant Colony Optimization algorithm (ACO). In this study, an attempt has been made to suggest a method to minimize weight and to improve the strength of the structure simultaneously.

In another study, a weight minimization has been performed in a hydrogen storage vessel using an adaptive genetic algorithm [6]. The burst pressure of the vessel was applied as a limitation load to design a composite vessel. Design variables were considered as thickness and angle of layers. Also, an investigation was conducted on the influence of the population size and the number of genetic algorithm parameters to reach an optimum outcome. In the following section, an optimization of the composite pressure vessels has been examined in a series of studies [7, 8].

In recent studies, the influence of numerous arrangements of stiffeners like triangular, square, semicircular, rectangular, circular etc. was analyzed by Ansys workbench. In this way, static and free vibrational analyses were performed. Ultimately, considering the parameters such as structural stiffness, von Mises stress, weight and deformation, the most efficient stiffener design was suggested [9, 10]. In the other pioneering study, shape optimization of axisymmetric pressure vessels was studied based on an integrated procedure, using a multi-objective function. It was employed for minimization of the von Mises stress from nozzle to head and what was finally obtained were completely different shapes from the usual ones [11].

In spite of a great number of studies on pressure vessels, it sounds that the optimization of end caps, especially flat ones, can be focused on potentially to reach novel outcomes. In this study, a comprehensive investigation of enormous-blunt end caps was performed under external pressure to reach the most efficient geometrical configuration. In the present study, numerous simulations were performed in a rather wide range of two definite geometrical parameters to determine an optimization state of stresses in a reinforced-flat end cap considering weight limitation. After constituting an objective function, an analytical study and also genetic algorithm were used to reach the most economic and efficient design. Moreover, a profound observation of the influence of two geometrical parameters was accomplished in different weight limits.

2. Geometry

A reinforced-flat end cap of 5800mm diameter was investigated in the present study. For particular conditions of installation site such as lack of sufficient space, employing other types of standard end caps was impractical. This flat end cap was an essential part of the designed main duct in the Air Cooled Condenser (ACC) system. In thermal power plants, an ACC is a configuration of cooling that brings about steam to be condensed inside a definite arrangement of finned tubes. The steam moves from the discharge of a steam turbine to the ACC where condensation happens. Subsequently, in a closed loop, the condensate goes back to the boiler. It is noteworthy that the sole purpose of ACC is conversion of hot steam to liquid water to prevent a waste of water and energy. A schematic view of designed ACC system is shown in Fig. 1. It shows a main duct that is closed horizontally through a reinforced-flat end cap, highlighted as an area of interest.

A better illustration of the simulated reinforced-flat end cap is presented in Fig. 2. As can be observed, it shows two parameters of height and thickness of stiffeners known as "h" and "t", respectively. Furthermore, applied external pressure and boundary conditions are shown which will be more elaborated in the next section.
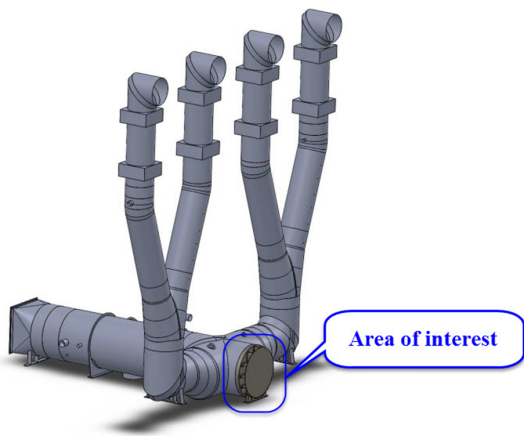
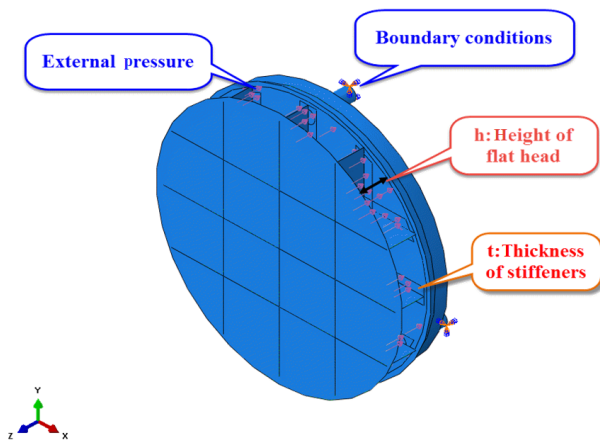**Fig. 1.** Area of interest in an ACC system.

Fig. 2. Two considered parameters to variate in a certain domain and the location of applied pressure and boundary conditions.

3. Finite Element Simulation

To simulate the reinforced-flat end cap under external pressure loading, ABAQUS commercial code [12] was employed. A number of simulations were carried out in order to encompass practical combinations of height and thickness of stiffener plates (hereafter called "h" and "t", respectively). In this way, "h" and "t" were assumed to vary between 300 to 900mm and 5 to 30mm, respectively. Although the considered range is based on the actual available space in the implemented power plant to prevent collision between the duct and other structures, the obtained results are applicable to all similar cases . RST 37 2 is used as applied material. Regarding allowable stresses considered in ASME Sec VIII div 1 as criteria, all pressure vessel designs shall be performed in a safe region which is far away enough compared to yield stress. Therefore, all simulations were conducted in an elastic zone. Table 1 demonstrates the material properties used in the current study.

Table 1
Applied mechanical properties.

Young modulus (GPa)	Poisson ratio
205	0.3

An isotropic hardening behavior was also assumed. Because of the asymmetrical geometry of the loading situation, the specimen was simulated in a complete model conforming to the original designed end cap.

A three dimensional shell extrude method was used as t and h can be adjusted easily to constitute different desirable geometries. The diameter of cap was set equal to 5800mm. All the degrees of freedom were limited across the three rods which were welded (see Fig. 2).
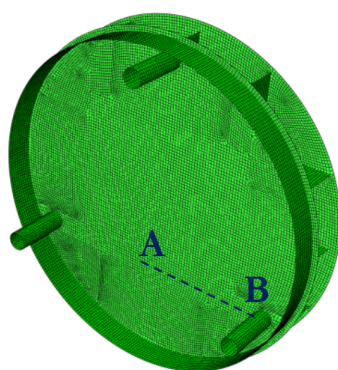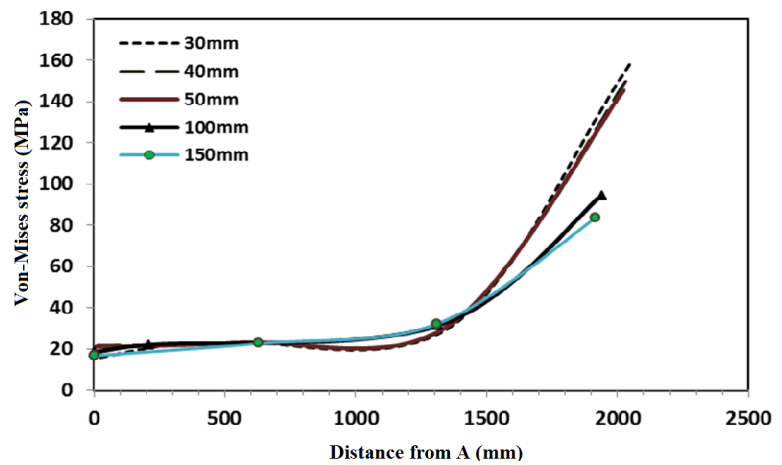
Fig. 3. Investigation of mesh element size influence, a) Typical path named as A-B for investigation, b) Von Mises stress through different mesh sizes.

The external pressure was applied equally to 1atm on the external face of end cap (see Fig. 2) which is equal to the maximum practical relative pressure difference between internal and external area of the duct. A 4-node doubly curved shell element called S4R was applied using reduced integration for all the simulations. Moreover, a comprehensive mesh convergence study was followed to reach an efficient element size. A typical study of convergence is shown in Fig. 3 across a path namely A-B shown in part (a). Fig. 3(b) illustrates von Mises stress obtained through the path including different mesh sizes. The maximum mesh sizes were considered equal to 30, 40, 50, 100 and 150mm. It is crystal clear that models with elements finer than 50mm will end in similar results. Thus, in order to optimize calculation time, maximum size of end cap elements was eventually set at 50mm.

Fig. 4(a) illustrates the obtained von Mises stress in a simulated flat end cap whose h and t were 700 and 5mm, respectively. Fig. 4(b) shows a detailed view of the critical region. As can be seen, the maximum stress was approximately equal to 280MPa, which has occurred at the root of the two symmetric rods as a support pipe. The similar pattern was found in all geometries. It seems to be a consequence of the external pressure that tends to bend the end cap inward and thus brings about the location of maximum stress in the bottom of the rods as principal obstacles against bending. It should be pointed out that, at the ultimate design, the maximum stress at the root of the rod was extremely reduced by means of sufficient welded-triangular stiffeners.

Upon completion of all the simulations, the desired information was extracted and as is discussed in the next section, they were utilized to form favorable-objective equation.

4. Model Clarification

In order to investigate each parameter's share on the induced stresses, a function of t and h was fitted to the obtained data through simulations as;

$$\frac{\sigma}{P} = f(x, y) \tag{1}$$

where σ is the maximum stress induced in the end cap, P is the applied external pressure; f is a polynomial equation fitted to the obtained data through numerical study; x and y are dimensionless forms of h and t, respectively, and were defined as:

$$x = \frac{h}{D}$$
$$y = \frac{t}{t_d} \tag{2}$$

where D and t_d are diameter and thickness of main duct, respectively, and f constituted a third-order equation formulated as Eq. (3):

$$f(x, y) = \sum_{j=0}^{3} \sum_{i=0}^{3} \alpha_{ij} x^i y^i \qquad i + j \leq 3 \tag{3}$$
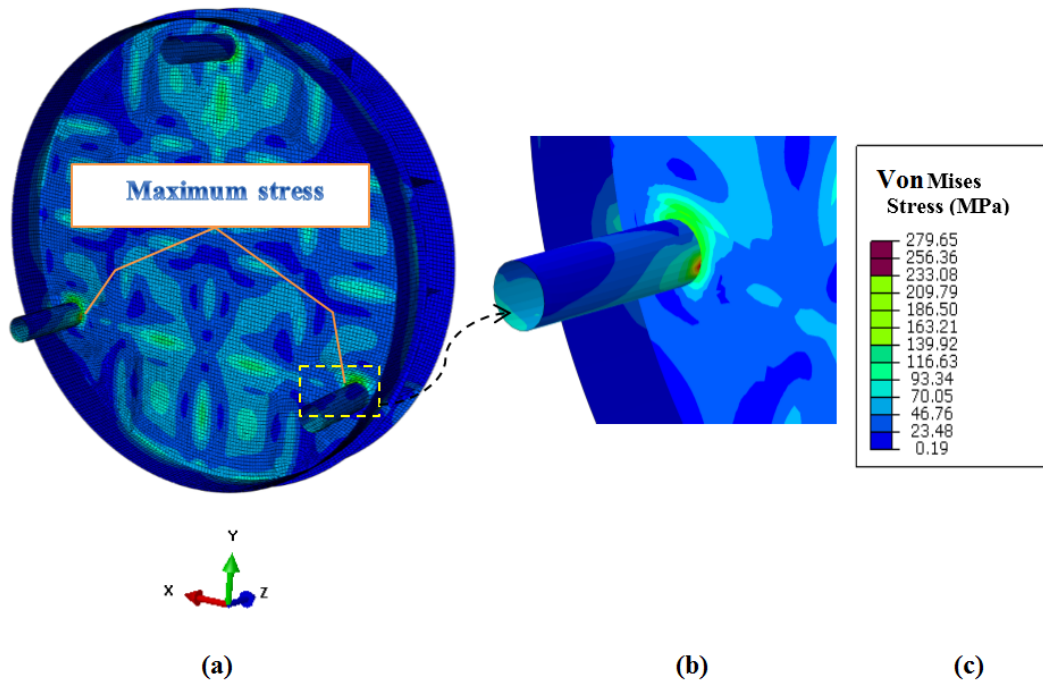
Fig. 4. a) A typical von Mises stress contour and the location in which maximum stress has occurred, b) Region of Maximum stress, c) Legend of contour.
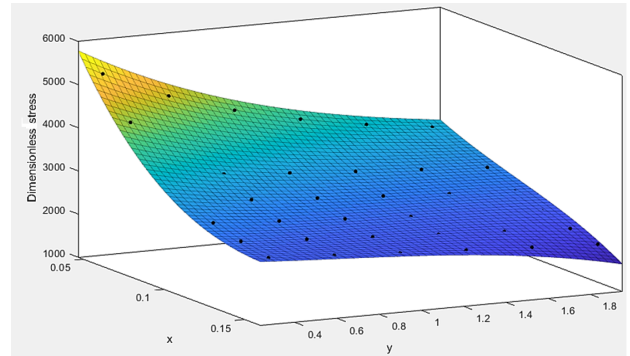
Table 2
Coefficients of Eq. (3).

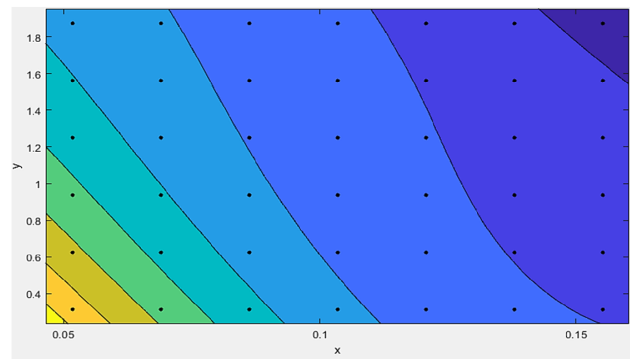| Coefficient	α_{00}	α_{10}	α_{01}	α_{20}	α_{11}	α_{02}	α_{30}	α_{21}	α_{12}	α_{03}
Magnitude	1.124e+04	-1.288e+05	-5687	6.11e+05	6.188e+04	1493	-9.017e+05	-1.817e+05	-7491	-161.9

In Eq. (3), α_{ij} is a functional coefficient shown in Table 2. This fitting has an R-squared item equal to 0.99 and residual average less than 1% that obviously shows how exact the fitted equation is. It is noteworthy that, based on the obtained residuals of fitted equations through a trial and error, 3rd-order polynomial equation had the least error compared with lower degrees. An equation with higher order could be used as well. However, it causes a more elaborate equation with approximately similar precision of 3rd-order equation.

It is also worth mentioning that, based on the π Buckingham theorem [13], all the used parameters were made dimensionless to avert confronting probable problems in the dimensions of the two sides of equations.

The contour of fitted surface to Eq. (1) is shown in Fig. 5(a). It is obvious that increasing h and t causes a reduction in stresses. A two-dimensional contour is also represented in Fig. 5(b) to provide more clarification. Regardless of the total end cap weight, the minimum stress is expected to appear at dusky zone (dark-violet region in right-up corner). Subsequently, for a constant weight, the most superior combination of h and t was obtained to attain the minimum stresses.

5. Optimization Model

In order to find an end cap with the least stresses induced on, the fitted function in previous section was employed. Furthermore, a relationship between weight and h and t was considered as a constraint to control the amount of material used in the structure. A linear precise function was defined as;

$$w = \sum_{i=1}^{1} \sum_{i=0}^{1} p_{ij} x^i y^j \qquad (4)$$

where p_{ij} are functional coefficients detailed in Table 3 and w is dimensionless form of weight defined as;

$$w = \frac{mg}{Pt_d^2} \qquad (5)$$

in which, m and g are the mass of flat end cap and gravitational acceleration (9.81m/s^2), respectively.

Table 3
Coefficients of Eq. (4).

Coefficient	p_{00}	p_{10}	p_{01}
Magnitude	1.124e+04	-1.288e+05	-5687

(a)

(b)

Fig. 5. a) The contour of fitted surface, b) Two-dimensional contour x versus y.
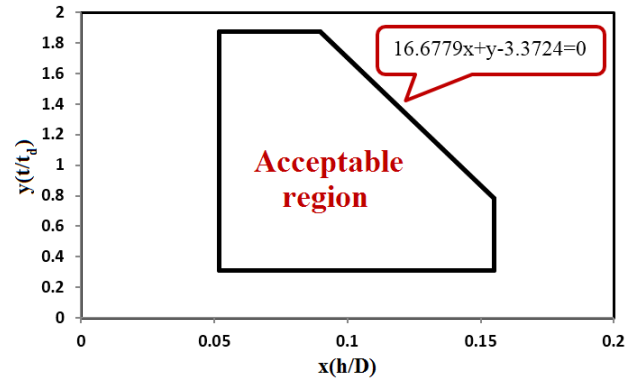
Fig. 6. The acceptable region for x and y given weight restriction.

Based on the desirable spring support to tolerate the weight of the designed-flat end cap, the maximum authorized mass was assumed equal to 16 tons. Allowable weight is determined according to the maximum limitation of certain types of spring support considered in the bottom of end cap to undergo weight loads. Therefore, according to Eq. (4), an added boundary condition was supposed as;

$$16.6779x + y \leq 3.3724 \qquad (6)$$

Fig. 6 shows all the considered boundary conditions to form an acceptable region. The inclined line determines the restriction caused by the maximum weight.

6. Analytical Study

6.1. Kuhn-Tucker Conditions

In nonlinear optimization problems, the Karush-Kuhn-Tucker (KKT) conditions should be satisfied for a local minimum candidate [14]. The KKT procedure for non-linearization of equations is through generalization of Lagrange multipliers, which is able to solve problems in the presence of inequality constraints. For instance, in order to minimize $f(x)$ regarding $g_i(x) \leq 0$ for $i = 1, 2, \cdots, m$, as boundary conditions, the KKT conditions for $X^* = [x_1^*\ x_2^*\ \cdots\ x_n^*]$ to be a local minimum are [14];

(a) $\dfrac{\partial f}{\partial x_i} + \sum\limits_{i=1}^{m} \mu_j \dfrac{\partial g}{\partial x_i} = 0 \qquad i = 1, 2, \cdots, n$

(b) $\mu_i g_i = 0 \qquad\qquad\qquad j = 1, 2, \cdots, m$ $\qquad$ (7)

(c) $g_i \leq 0 \qquad\qquad\qquad\ j = 1, 2, \cdots, n$

(d) $\mu_j \geq 0 \qquad\qquad\qquad\ j = 1, 2, \cdots, m$

6.2. Solution

With regard to Eq. (3) in the current problem, the KKT conditions are listed in Table 4.

Based on these conditions, 14 different cases were considered, each of which was potentially a candidate of local minimum. The final results are also shown in Table 5 in a nutshell.

As can be observed in Table 5, the sole case that has satisfied all KKT conditions was case 3. In this case, the maximum stress obtained was equal to 236MPa. As can be seen in the next section, Genetic Algorithm (GA) has also confirmed this minimum stress point.

7. Genetic Algorithm

As a powerful technique, GA is able to get to the bottom of an optimization question even complicated problems, and also those ones that are difficult to obtain an exact solution analytically [15, 16]. A GA is a progressive algorithm based on natural evolution procedure to find an optimum result through an acceptable domain. A random "population" using acceptable region is made at first. Subsequently, over the next generation of the individuals, the algorithm tries to extract new members that are more appropriate in comparison with previous ones. Hence, each iteration procedure generally leads to the improvement of the answers, and it is expected that the best solution would be derived after the accomplishment of the algorithm [17].

"Crossover" and "mutation" are two frequent ways to create new generations. In crossover, a certain selection pressure is used to pick out two individuals as parents through former step. Merging genes of parents can breed new individuals as "offspring". Note that using the sole crossover would lead to extracting local minimums.

In order to ensure certain exploration in the entire acceptable region, mutation was employed as another operator with less contribution. Note that excessive usage of mutation may prevent convergence [17].

Table 4
KKT conditions for current matter.

Condition	Group
$e_1 : p_{10} + 2p_{20}x + p_{11}y + 3p_{30}x^2 + 2p_{21}xy + p_{12}y^2 + \mu_1 - \mu_2 + 16.678\mu_5 = 0$ $e_2 : p_{01} + p_{11}x + 2p_{02}y + p_{21}x^2 + 2p_{12}xy + 3p_{03}y^2 + \mu_3 - \mu_4 + \mu_5 = 0$	(a)
$e_3 : \mu_1(x - 0.1552) = 0$ $e_4 : \mu_2(0.0517 - x) = 0$ $e_5 : \mu_3(y - 1.875) = 0$ $e_6; \mu_4(0.312 - y) = 0$ $e_7 : \mu_5(16.678x + y - 3.3724) = 0$	(b)
$e_8 : x - 0.1552 \leq 0$ $e_9 : 0.0517 - x \leq 0$ $e_{10} : y - 1.875 \leq 0$ $e_{11} : 0.312 - y \leq 0$ $e_{12} : 16.678x + y - 3.373 \leq 0$	(c)
$e_{13} : \mu_1 \geq 0$ $e_{14} : \mu_2 \geq 0$ $e_{15} : \mu_3 \geq 0$ $e_{16} : \mu_4 \geq 0$ $e_{17} : \mu_5 \geq 0$	(d)

Table 5
Investigation of different cases to reach minimum candidate.

Case No.	Assumptions	Subsequent assumptions	Results	Acceptable/ unacceptable
1	$x = 0.1552 \ y = 1.875$	$\mu_2 = \mu_4 = \mu_5 = 0$	$e_{12} : 1.091 > 0$	unacceptable
2	$x = 0.1552 \ y = 0.312$	$\mu_2 = \mu_3 = \mu_5 = 0$	$e_2 : \mu_4 = -301 < 0$	unacceptable
3	$x = 0.1552$	$\mu_2 = \mu_3 = \mu_4 = 0$	$e_7 : y = 0.784$ $e_1 : \mu_1 = 603.5$ $e_2 : \mu_5 = 240.3$	acceptable
4	$x = 0.1552$	$\mu_2 = \mu_3 = \mu_4 = \mu_5 = 0$	$e_2 : y = 0.272, 3.48 \rightarrow$ Not in acceptable range	unacceptable
5	$x = 0.0517, \ y = 1.875$	$\mu_1 = \mu_4 = \mu_5 = 0$	$e_1 : \mu_2 = -18390.7$	unacceptable
6	$x = 0.0517, \ y = 0.312$	$\mu_1 = \mu_3 = \mu_5 = 0$	$e_1 : \mu_2 = -60137.5 < 0$ $e_2 : \mu_4 = -2330.78 < 0$	unacceptable
7	$x = 0.0517$	$\mu_1 = \mu_3 = \mu_4 = 0$	$e_{12} : y = 2.51$ $e_1 : \mu_2 = -3833.5 < 0$ $e_2 : \mu_5 = 482.76$	unacceptable
8	$x = 0.0517$	$\mu_1 = \mu_3 = \mu_4 = \mu_5 = 0$	(8.1) if $y = 1.658 \rightarrow$ $e_1 : \mu_2 = -21998.6$ (8.2) if $y = 3.693 \rightarrow$ Not in acceptable range	unacceptable
9	$y = 1.875$	$\mu_1 = \mu_2 = \mu_4 = 0$	$e_{12} : x = 0.089$ $e_1 : \mu_5 = 744.8$ $e_2 : \mu_3 = -517 < 0$	unacceptable
10	$y = 1.875$	$\mu_1 = \mu_2 = \mu_4 = \mu_5 = 0$	e_1: No real answer for x	unacceptable
11	$y = 0.312$	$\mu_1 = \mu_2 = \mu_3 = 0$	$e_{12} : x = 0.1835$ Not in acceptable range	unacceptable
12	$y = 0.312$	$\mu_1 = \mu_2 = \mu_3 = \mu_5 = 0$	(12.1) if $x = 0.1697 \rightarrow$ Not in acceptable range (12.2) if $x = 0.24 \rightarrow$ $e_{12} = 0.94 > 0$	unacceptable
13	$\mu_1 = \mu_2 = \mu_3 = \mu_4 = 0$	−	e_{12}, e_1 and $e_2 \rightarrow x = 0.1661$ or $x = -1.4127$ Not in acceptable range	unacceptable
14	$\mu_1 = \mu_2 = \mu_3 = \mu_4 = \mu_5 = 0$	−	Obtained x and y are not in acceptable range	unacceptable

In the present optimization, h and t, in dimensionless form, were assumed as design variables. Variable acceptable ranges and variation domain of t and h were considered as what is shown in Fig. 6. They were determined through optimization of Eq. (1). Acceptable region was also considered to be what is shown in Fig. 6. The final result was perfectly in compliance with those anticipated by analytical study.

8. Results

Given an extent for weight of end cap, a combination of h and t has been obtained through analytical method and GA simultaneously. This was done using four other weight restrictions. These restrictions were assumed as 15, 15.5, 16.5 and 17 tons. The acceptable region and optimum point are represented in Fig. 7 in each case. Note that, in this figure, the inclined-dash lines show boundaries created by limitations in weight. It can be observed clearly that h is more influential than t in terms of reducing stress induced in the end cap. In other words, for a definite weight, the end cap with the largest h will be more appropriate than other possible cases. It can be justified through bending moments that are dominant type of normal stresses created by external pressure. These moments tend to bend the end cap inward. As can be seen in Fig. 4, maximum stresses have appeared at locations with maximum bending stresses. Based on the strength of material science, there is a conventional relationship for bending stresses $\left(\sigma = \dfrac{Mc}{I} \right)$ that confirms that a growth at h effectively increases moment of inertia at a faster pace (the denominator of recent equation) and subsequently brings about a great reduction in bending stresses.

Furthermore, maximum induced stresses have been

observed through different weight restrictions at optimal points. The results are accounted for in Fig. 8. As can be observed, the stresses have been plunged exponentially approximately 27% from 15 to 15.5 tons. Subsequently, the changes up to 17 tons tend to reduce stress linearly at a rather slow rate. It means that using stronger material, typically with higher yield stress, is able to compensate for the lack of safety due to mass reduction. Note that this recommendation can be applied only if possible and also affordable.
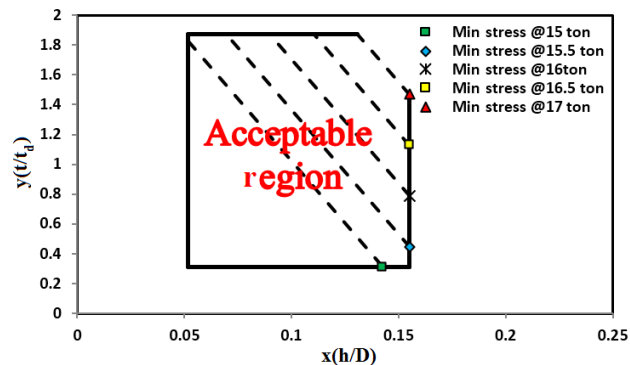

Fig. 7. Acceptable region and minimum stress point in 5 different weight restrictions.
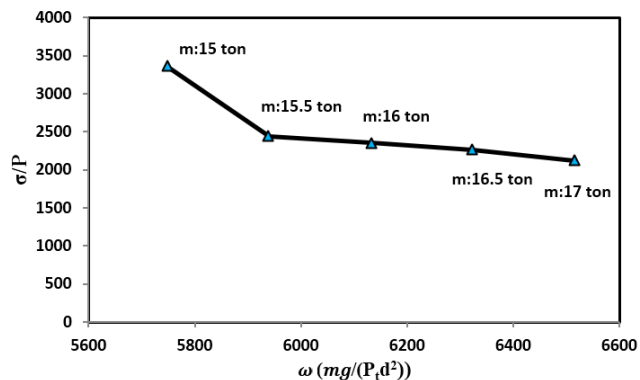

Fig. 8. Maximum induced stress versus different weight restriction.

9. Discussion and Concluding Remarks

A general investigation of the reinforced end cap of an enormous pressure vessel under external pressure has been performed in this study. An array of constant-diameter flat end caps at different h and t were simulated to observe the obtained trends. Subsequently, a function was fitted to the results to extract objective function. Moreover, favorable boundary conditions were considered using a limitation for weight of the end cap. An analytical study and also GA were implemented to find an end cap that has the most economic and efficient design simultaneously. As was noted, for a certain weight, the end cap with the largest h was more appropriate than other possible cases. A comprehensive observation of the influence of the two

geometrical parameters was accomplished in different weight limits as well. It was found that although increasing the weight generally reduces stresses; there is a point beyond which the weight growth becomes less effective. Overall, this research proposes an exact procedure to reduce the induced stresses under external pressure.

All in all, the findings in a nutshell are:

- Optimization of a huge duct under external pressure

- A rather extensive finite element study of blunt end caps

- Investigation of the impression of each geometrical factor

- A perfect compliance between analytical and GA method

10. Acknowledgement

References

[1] D.R. Moss, M. Basic, Pressure Vessels Design, Oxford, UK: Elsevier Inc., (2013).

[2] A.H. Mahmoudi, A.R. Hosseinzadeh, M. Jooya, Plasticity effect on residual stresses measurement using contour method, Int. J. Eng. 26(10) (2013) 1203-1212.

[3] A.T. Poojary, R.S. Sharma, M.H. Patel, D.U. Sheth, C.R. Kini, R. Nayak, Design and modelling of hemispherical and flat dish end pressure vessel, Indian J. Sci. Technol., 8(33) (2015) 1-7.

[4] G. Towler, R. Sinnott, Chemical Engineering Design: Principles, Practice and Economics of Plant and Process Design, Boston: Elsevier, (2013).

[5] S. Hassan, K. Kumar, Ch.D. Raj, K. Sridhar, Design and optimisation of pressure vessel using metaheuristic approach, Appl. Mech. Mater., 465-466 (2014) 401-406.

[6] P. Xu, J. Zheng, H. Chen, P. Liu, Optimal design of high pressure hydrogen storage vessel using an adaptive genetic algorithm, Int. J. Hydrog. Energy, 35(7) (2010) 2840-2846.

[7] C.P. Fowler, A.C. Orifici, C.H. Wang, A review of toroidal composite pressure vessel optimization and damage tolerant design for high pressure gaseous fuel storage, Int. J. Hydrog. Energy, 41(47) (2016) 22067-22089.

[8] D. Leh, B. Magneville, P. Saffr, P. Francescato, R. Arrieux, S. Villalonga, Optimization of 700 bar type IV hydrogen pressure vessel considering composite damage and dome multi-sequencing, Int. J. Hydrog. Energy, 40(38) (2015) 13215-13230.

[9] A.E. Kumar, R.K. Santosh, S.R. Teja, E. Abishek, Static and dynamic analysis of pressure vessels with various, Materials Today: Proceedings, 5(2) (2018) 5039-5048.

[10] B.S. Kumar, P. Prasanna, J. Sushma, K.P. Srikanth, Stress analysis and design optimization of a pressure vessel using Ansys package, Materials Today: Proceedings, 5 (2018) 4551-4562.

[11] R.C. Carbonari, P.A. Muñoz-Rojas, E.Q. Andrade, G.H. Paulino, K. Nishimoto, E.C.N. Silva, Design of pressure vessels using shape optimization: An integrated approach Carbonari, Int. J. Press. Vessels Pip., 88(5-7) (2011) 198-212.

[12] ABAQUS 6.14, User's Manual, ABAQUS, (2014).

[13] E. Buckingham, On physically similar systems; illustrations of the use of dimensional equations, Phys. Rev., 4(4) (1914) 345-376.

[14] R.K. Arora, Optimization algorithms and applications, Trivandrum, India: Chapman and Hall/CRC, (2015).

[15] A.R. Hosseinzadeh, A.H. Mahmoudi, Determination of mechanical properties using sharp macro-indentation method and genetic algorithm, Mech. Mater., 114 (2017) 57-68.

[16] A.R. Hosseinzadeh, A.H. Mahmoudi, Measuring non-equi biaxial residual stresses and material properties using Knoop indentation, J. Test. Eval., 48(2) (In Press), DOI: 10.1520/JTE20170730.

[17] M. Melanie, An Introduction to Genetic Algorithms, Cambridge, Massachusetts: Massachusetts Institute of Technology, (1999).